20140701IA

厚生労働科学研究費補助金

創薬基盤推進研究事業

認知症/神経変性疾患モデルショウジョウバエバンクの構築と変性蛋白質オリゴマーを標的とした共通の治療薬開発

（H24－創薬総合－一般－002）

平成２６年度　総括研究報告書

研究代表者　永井　義隆

平成２７（２０１５）年　５月

厚生労働科学研究費補助金

創薬基盤推進研究事業

認知症/神経変性疾患モデルショウジョウバエバンクの構築と変性蛋白質オリゴマーを標的とした共通の治療薬開発

（H24－創薬総合－一般－002）

平成２６年度　総括研究報告書

研究代表者　永井　義隆

平成２７（２０１５）年　５月

目　　次

厚生労働科学研究費補助金(創薬基盤推進　研究事業)
総括研究報告

認知症/神経変性疾患モデルショウジョウバエバンクの構築と変性蛋白質オリゴマーを標的とした共通の治療薬開発

研究代表者　永井 義隆（国立精神・神経医療研究センター神経研究所疾病研究第四部）

研究要旨

近年、アルツハイマー病（AD）、パーキンソン病（PD）、ポリグルタミン（PolyQ）病など多くの認知症/神経変性疾患では、それぞれ異なる変性蛋白質のオリゴマー重合体により共通に神経変性が惹き起こされると考えられている。私たちはこれまで変性蛋白質オリゴマーを標的とした共通の治療薬開発研究を進め、*in vitro* アッセイ系を用いた1次スクリーニングにより PolyQ 蛋白質のオリゴマー阻害化合物を約 100 種類同定している。本研究では、このような治療薬候補化合物の迅速・簡便な *in vivo* での薬効評価に適するハイスループット動物モデルとして、1）疾患ショウジョウバエモデルバンクを樹立し、2）認知症/神経変性疾患の分子標的治療薬を創薬することを目的として研究を行った。その結果、1）疾患モデルショウジョウバエバンクの保有系統数は、研究開始時点の 46 系統から 118 系統の樹立・収集を完了した。2）1次ヒットオリゴマー阻害化合物から、血液脳関門透過性・安全性が高い治療薬候補 QX1 について、PolyQ 病モデルマウスの脳内 PolyQ 凝集体の抑制効果を認めた。一方、QX1 が Amyloid-β の凝集阻害活性も発揮することを明らかにしたが、AD などの疾患モデルショウジョウバエ、AD モデルマウスに対する有効性は明らかではなかった。

A. 研究目的

加齢に伴って発症する認知症/神経変性疾患の克服は、我が国の厚生労働行政上重要な課題である。近年、アルツハイマー病、パーキンソン病、ポリグルタミン病など多くの認知症/神経変性疾患では、様々な変性蛋白質のオリゴマー重合体により共通に神経変性が惹き起こされると考えられている。私たちはこれまで変性蛋白質オリゴマーを標的とした共通の治療薬開発研究を進め、*in vitro* アッセイ系を用いた1次スクリーニングにより大規模化合物ライブラリー（約 45,000 化合物）から約 100 種類の新規オリゴマー阻害化合物を同定している。

本研究では、このような治療薬候補化合物の迅速・簡便な *in vivo* での薬効評価に適する疾患ショウジョウバエモデルバンクを樹立し、認知症/神経変性疾患の分子標的治療薬を創薬することを目的として、以下の研究を行った。

B&C&D. 研究方法・結果および考察

1）認知症/神経変性疾患モデルショウジョウバエバンクの構築：

認知症/神経変性疾患関連遺伝子を過剰発現、あるいは RNAi 法により各遺伝子の発現をノックダウンするトランスジェニックショウジョウバエの作製・入手を進めた。

研究開始時点で合計 46 系統の疾患モデルショウジョウバエを保有し、H24 年度から新規疾患モデルショウジョウバエの作製・樹立を進め、H25 年度末までに、アルツハイマー病（AD）：9 系統、前頭側頭葉型認知症（FTD）：6 系統、パーキンソン病（PD）：27 系統、筋萎縮性側索硬化症（ALS）：34 系統、ポリグルタミン（PolyQ）病： 21 系統、その他： 9 系統の合計 106 系統とした。

H26 年度は ALS: 11 系統、その他： 1 系統の疾患モデルショウジョウバエを作製・入手し、合計 118 系統とした（H26 年度目標 110 系統）。

2）新規オリゴマー阻害化合物の疾患モデルショウジョウバエ/マウスを用いたハイスループット薬効評価による治療薬開発：

研究開始時点で同定していた約 100 種類の1次ヒット PolyQ 蛋白質オリゴマー阻害化合物うち、H24-25 年度に入手可能であった 14 種類のうち、PolyQ 病モデルショウジョウバエの複眼変性の抑制効果を認める 8 化合物を同定した。そして、PolyQ 蛋白質だけでなく、Amyloid-β、Tau、α-Synuclein などの変性蛋白質のオリゴマー阻害活性を発揮し、PolyQ 病、AD、PD いずれの疾患モデルショウジョウバエの複眼変性も抑制する化合物 QX2 を同定した。さらに、PolyQ 病モデルショウジョウバエへの有効性を確認し、血液脳関門透過性・安全性が高い治療薬候補 QX1 については、脊髄小脳失調症1型モデル SCA1-Q154 と球脊髄性筋萎縮症モデル AR-Q97 の2つの PolyQ 病モデルの運動障害を有意に改善することを明らかにし

た。

H26年度は、治療薬候補QX1について、PolyQ病モデルマウスの脳内PolyQ凝集体に対する影響を検討した。その結果、QX1の経口投与により、SCA1-Q154モデルマウスの脳内PolyQ凝集体形成が有意に抑制されることを明らかにした。

また、QX1のPolyQ病以外の他の神経変性疾患原因蛋白質、AD、FTD、PD、ALSなどの疾患モデルに対する治療効果を検討した。その結果、QX1はPolyQ蛋白質だけでなく、Amyloid-βの凝集阻害活性も発揮することを明らかにした。しかしながら、QX1はAD、FTD、PD、ALSの疾患モデルショウジョウバエに対しては、いずれの複眼変性にも有意な抑制効果を示さなかった。さらに、ADモデルマウスAPPswe/PS1 dE9を用いて、QX1経口投与による薬効評価を行ったが、Thioflavin S染色の結果、ADモデルマウス脳内のアミロイド斑の有意な抑制効果を認めなかった。

（倫理面への配慮）

本研究では直接ヒトを対象とした研究は行っていない。

E. 結論

本研究の結果から、*in vitro* アッセイ系から得られた新規オリゴマー阻害化合物の迅速・簡便な*in vivo*での薬効評価として疾患モデルショウジョウバエ有用であることが確認され、今後、QX1をはじめとした疾患モデルマウスで有効性を示す薬剤の同定が期待される。

F. 健康危険情報

なし

G. 研究発表

1．論文発表

1) Takeuchi T., Suzuki M., Fujikake N., Popiel H.A., Kikuchi H., Futaki S., Wada K., *Nagai Y. Intercellular chaperone transmission via exosomes contributes to maintenance of protein homeostasis at the multicellular organismal level. ***Proc. Natl. Acad. Sci. USA.*** (in press)
2) Takahashi M., Suzuki M., Fukuoka M., Fujikake N., Watanabe S., Murata M., Wada K., Nagai Y., Hohjoh H. Normalization of overexpressed α-synuclein causing Parkinson's disease by a moderate gene silencing with RNA interference. ***Mol. Ther. Nucleic Acids*** (in press)
3) Saitoh Y., Fujikake N., Okamoto Y., Popiel H.A., Hatanaka Y., Ueyama M., Suzuki M., Gaumer S., Murata M., Wada K., *Nagai Y. p62 plays a protective role in the autophagic clearance of polyglutamine aggregates in polyglutamine disease model flies. ***J. Biol. Chem.*** 290(3): 1442-1453 (2015)
4) Miura E., Hasegawa T., Konno M., Suzuki M., Sugeno N., Fujikake N., Geisler S., Tabuchi M., Oshima R., Kikuchi A., Baba T., Wada K., Nagai Y., Takeda A., Aoki M. VPS35 dysfunction causes retromer depletion and impairs lysosomal degradation of α-synuclein, leading to exacerbation of α-synuclein neurotoxicity in *Drosophila*. ***Neurobiol. Dis.*** 71: 1-13 (2014)
5) Azuma Y., Tokuda T., Shimamura M., Kyotani A., Sasayama H., Yoshida T., Mizuta I., Mizuno T., Nakagawa M., Fujikake N., Ueyama M., Nagai Y., Yamaguchi M. Identification of *ter94*, *Drosophila VCP*, as a strong modulator of motor neuron degeneration induced by knockdown of *Caz*, *Drosophila FUS*. ***Hum. Mol. Genet.*** 23(13): 3467-3480 (2014)
6) Takeuchi T., Popiel H.A., Futaki S., Wada K., *Nagai Y. Peptide-based therapeutic approaches for treatment of the polyglutamine diseases. ***Curr. Med. Chem.*** 21(23): 2575-2582 (2014)
7) 上山盛夫、藤掛伸宏、永井義隆. その他のFTLD—異常蛋白の視点から. ***Clinical Neuroscience*** 33 (3): 312-314 (2015)
8) 永井義隆. ポリグルタミン病における神経変性. ***BRAIN MEDICAL*** 26 (3): 225-229 (2014)

2．学会発表

1) Nagai Y. Misfolding and aggregation of the polyglutamine protein and its suppression by intercellular transmission of molecular chaperone. ***Hungary-Japanese Symp on Mechanism and regulation of aberrant protein aggregation*** (Nov 17-21, 2014, Osaka, Japan)
2) Minakawa et al. Investigating the role of ubiquilin-2 in the pathomechanism of ALS/FTD. ***GRC on Neurobiol Brain Dis*** (Jul 27-Aug 1, 2014, Girona, Spain)
3) Nagai Y., et al. Dysfunction of microtubule- dependent transport triggers oligomerization and cytoplasmic accumulation of TDP-43, leading to neurodegeneration. ***CSHL 2014 Neurodeg Dis meeting*** (Dec 3-6, 2014, CSH, NY, USA)
4) Saitoh Y., et al. p62 plays a protective role in the autophagic degradation of polyglutamine protein oligomers in polyglutamine disease model flies. ***CSHL 2014 Neurodeg Dis meeting*** (Dec 3-6, 2014, CSH, NY, USA)
5) Ishiguro T., et al. Expanded UGGAA repeat RNA associated with SCA31 causes progressive neurodegeneration in *Drosophila*. ***CSHL 2014 Neurodeg Dis meeting*** (Dec 3-6, 2014, CSH, NY, USA)
6) 永井義隆、他. ２光子in vivoイメージング解析による SCA1 マウスにおけるシナプス異常の解明. ***第 55 回 日本神経学会学術大会*** (H26.5.21-24、福岡)
7) 藤掛伸宏、他. DCTN1依存的輸送の障害はTDP-43のオリゴマー形成を促進する. ***第 55 回 日本神経学会学術大会*** (H26.5.21-24、福岡)
8) 鈴木マリ、他. ポリグルタミン病モデルショウジョウバエの神経変性は過栄養摂取により増悪す

る．*第55回 日本神経学会学術大会*（H26.5.21-24、福岡）
9) 斉藤勇二、他．ポリグルタミン病モデルにおいてp62 はオートファジー分解系を介して保護的に作用する．*第 55 回 日本神経学会学術大会*（H26.5.21-24、福岡）
10) Minakawa E.N., et al. Investigating the Role of Ubiquilin-2 in the Pathomechanism of ALS/FTD. *第55回 日本神経学会学術大会*（H26.5.21-24、福岡）
11) 東裕美子、他．FUS-ALS モデルショウジョウバエの表現型を修飾する因子の探索．*第 55 回 日本神経学会学術大会*（H26.5.21-24、福岡）
12) 三浦永美子、他．VPS35 障害はカテプシン D 活性低下を介しαシヌクレイン蓄積・神経変性を惹起する．*第55回 日本神経学会学術大会*(H26.5.21-24、福岡)
13) 石黒太郎、他．SCA31 (UGGAA)n リピートはショウジョウバエで進行性神経障害を引き起こす．*第55回 日本神経学会学術大会*（H26.5.21-24、福岡）
14) 鈴木マリ、他．神経変性疾患モデルショウジョウバエの神経変性は過栄養摂取により増悪する．*第37回 日本神経科学会*（H26.9.11-13、横浜）
15) 斉藤勇二、他．p62/SQSTM1 はポリグルタミン病モデルショウジョウバエにおいて、ポリグルタミン蛋白質凝集体をオートファジー分解系で除去することで保護的役割を果たす．*第 37 回 日本神経科学会*（H26.9.11-13、横浜）
16) Minakawa et al. Investigating the role of ubiquilin-2 in the pathomechanism of ALS/FTD. *第37回 日本神経科学会*（H26.9.11-13、横浜）
17) 石黒太郎、他．異常伸長 UGGAA リピート RNA はショウジョウバエにおいて神経毒性を引き起こす．*第37回 日本神経科学会*（H26.9.11-13、横浜）
18) 上山盛夫、他．GGGGCC リピート RNA を発現する新規 ALS モデルショウジョウバエの樹立と病態解析．*第 86 回 日本遺伝学会大会*（H26.9.17-19、長浜）
19) 永井義隆、他．微小管依存的 TDP-43 輸送の障害はオリゴマー形成を促進し、神経変性を惹き起こす．*第33回 日本認知症学会学術集会*(H26.11.29-12.1、横浜)

H. 知的財産権の出願・登録状況（予定を含む。）

1) 発明者名：石川欽也、水澤英洋、永井義隆、横田隆徳、石黒太郎、佐藤望、和田圭司
発明の名称：ALS の原因タンパク毒性を軽減する核酸
特許出願番号：特願 2014-244034
出願日：2014 年 12 月 2 日
出願人：東京医科歯科大学、国立精神・神経医療研究センター
2) 発明者名：石川欽也、水澤英洋、永井義隆、石黒太郎、佐藤望、和田圭司
発明の名称：脊髄小脳失調症 31 型（SCA31 治療剤
特許出願番号：特願 2014-244350
出願日：2014 年 12 月 2 日
出願人：東京医科歯科大学、国立精神・神経医療研究センター
3) 発明者名：武内敏秀、永井義隆、中川慎介、丹羽正美、道具伸也、片岡泰文、高田芙友子
発明の名称：血液脳関門透過性ペプチド
特許出願番号：特願 2015-052967
出願日：2015 年 3 月 17 日
出願人：京都大学、国立精神・神経医療研究センター、長崎大学・ファーマコセル株式会社、福岡大学

研究成果の刊行に関する一覧表

書籍

著者氏名	論文タイトル名	書籍全体の編集者名	書　籍　名	出版社名	出版地	出版年	ページ

雑誌

発表者氏名	論文タイトル名	発表誌名	巻号	ページ	出版年
Takeuchi T., Suzuki M., Fujikake N., Popiel H.A., Kikuchi H., Futaki S., Wada K., *Nagai Y.	Intercellular chaperone transmission via exosomes contributes to maintenance of protein homeostasis at the multicellular organismal level.	Proc. Natl. Acad. Sci. USA.			in press
Takahashi M., Suzuki M., Fukuoka M., Fujikake N., Watanabe S., Murata M., Wada K., Nagai Y., Hohjoh H.	Normalization of overexpressed α-synuclein causing Parkinson's disease by a moderate gene silencing with RNA interference.	Mol. Ther. Nucleic Acids.			in press
Saitoh Y., Fujikake N., Okamoto Y., Popiel H.A., Hatanaka Y., Ueyama M., Suzuki M., Gaumer S., Murata M., Wada K., *Nagai Y.	p62 plays a protective role in the autophagic clearance of polyglutamine aggregates in polyglutamine disease model flies.	J. Biol. Chem.	290 (3)	1442-1453	2015
Miura E., Hasegawa T., Konno M., Suzuki M., Sugeno N., Fujikake N., Geisler S., Tabuchi M., Oshima R., Kikuchi A., Baba T., Wada K., Nagai Y., Takeda A., Aoki M.	VPS35 dysfunction causes retromer depletion and impairs lysosomal degradation of α-synuclein, leading to exacerbation of α-synuclein neurotoxicity in *Drosophila*.	Neurobiol. Dis.	71	1-13	2014
Azuma Y., Tokuda T., Shimamura M., Kyotani A., Sasayama H., Yoshida T., Mizuta I., Mizuno T., Nakagawa M., Fujikake N., Ueyama M., Nagai Y., Yamaguchi M.	Identification of *ter94*, *Drosophila VCP*, as a strong modulator of motor neuron degeneration induced by knockdown of *Caz*, *Drosophila FUS*.	Hum. Mol. Genet.	23 (13)	3467-3480	2014
Takeuchi T., Popiel H.A., Futaki S., Wada K., *Nagai Y.	Peptide-based therapeutic approaches for treatment of the polyglutamine diseases.	Curr. Med. Chem.	21 (23)	2575-2582	2014
上山盛夫、藤掛伸宏、永井義隆	その他のFTLD―異常蛋白の視点から	Clinical Neuroscience	33 (3)	312-314	2015

永井義隆	ポリグルタミン病における神経変性	BRAIN MEDICAL	26 (3)	225-229	2014

研究成果の刊行物・別刷

Intercellular chaperone transmission via exosomes contributes to maintenance of protein homeostasis at the organismal level

Toshihide Takeuchi[a,b], Mari Suzuki[a], Nobuhiro Fujikake[a], H. Akiko Popiel[a], Hisae Kikuchi[a], Shiroh Futaki[b], Keiji Wada[a], and Yoshitaka Nagai[a,c,1]

[a]Department of Degenerative Neurological Diseases, National Institute of Neuroscience, National Center of Neurology and Psychiatry, Kodaira, Tokyo 187-8502, Japan; [b]Institute for Chemical Research, Kyoto University, Uji, Kyoto 611-0011, Japan; and [c]Core Research for Evolutional Science and Technology (CREST), Japan Science and Technology Agency, Kawaguchi, Saitama 332-0012, Japan

Edited by Nancy M. Bonini, University of Pennsylvania, Philadelphia, PA, and approved March 24, 2015 (received for review July 4, 2014)

The heat shock response (HSR), a transcriptional response that up-regulates molecular chaperones upon heat shock, is necessary for cell survival in a stressful environment to maintain protein homeostasis (proteostasis). However, there is accumulating evidence that the HSR does not ubiquitously occur under stress conditions, but largely depends on the cell types. Despite such imbalanced HSR among different cells and tissues, molecular mechanisms by which multicellular organisms maintain their global proteostasis have remained poorly understood. Here, we report that proteostasis can be maintained by molecular chaperones not only in a cell-autonomous manner but also in a non–cell-autonomous manner. We found that elevated expression of molecular chaperones, such as Hsp40 and Hsp70, in a group of cells improves proteostasis in other groups of cells, both in cultured cells and in *Drosophila* expressing aggregation-prone polyglutamine proteins. We also found that Hsp40, as well as Hsp70 and Hsp90, is physiologically secreted from cells via exosomes, and that the J domain at the N terminus is responsible for its exosome-mediated secretion. Addition of Hsp40/Hsp70-containing exosomes to the culture medium of the polyglutamine-expressing cells results in efficient suppression of inclusion body formation, indicating that molecular chaperones non-cell autonomously improve the protein-folding environment via exosome-mediated transmission. Our study reveals that intercellular chaperone transmission mediated by exosomes is a novel molecular mechanism for non–cell-autonomous maintenance of organismal proteostasis that could functionally compensate for the imbalanced state of the HSR among different cells, and also provides a novel physiological role of exosomes that contributes to maintenance of organismal proteostasis.

molecular chaperones | proteostasis | exosome | non-cell autonomous | polyglutamine

Molecular chaperones are protective molecules that are necessary for cell survival in stressful environments, which function to maintain protein homeostasis (proteostasis) (1). Upon exposure to various types of cellular stresses, such as heat, oxidative stress, or the intracellular accumulation of misfolded proteins, the expression of molecular chaperones, including heat shock proteins (HSPs), is rapidly up-regulated by the activation of heat shock transcription factors (HSFs) (2). HSPs typically bind to proteins with nonnative or denatured conformations and assist the proper folding of such proteins to prevent their aggregation (3, 4). The inability to maintain cellular proteostasis is likely to result in deleterious consequences, including protein conformation diseases, such as Alzheimer's disease, Parkinson's disease, and the polyglutamine diseases (5–8).

Although molecular chaperones are essential for cell survival, the heat shock response (HSR), a transcriptional response that up-regulates these chaperones upon heat stress, is not ubiquitously maintained in all cells and tissues, but occurs in a cell type-specific manner (9, 10). Whereas cerebellar neurons and glial cells show vigorous transcriptional up-regulation of heat shock genes upon exposure to stress, hippocampal neurons show less or almost no such response (11). The absence of chaperone expression up-regulation has also been observed in several types of cultured cells, which was directly linked to their enhanced vulnerability to various types of proteotoxic stresses (12, 13). Despite such imbalanced transcriptional responses of chaperone expression against proteotoxic challenges among different cells and tissues, the molecular mechanisms by which multicellular organisms maintain their global proteostasis have remained poorly understood.

In our previous study, viral vector-mediated heat shock protein Hsp40 (DnaJB1) overexpression in the brain of a polyglutamine disease mouse model unexpectedly suppressed inclusion body formation even in the virus-noninfected cells, in addition to the virus-infected cells (14), implying that elevated levels of chaperone expression in one group of cells might affect proteostasis in other groups of cells. We here provide direct evidence that proteostasis is indeed non-cell autonomously maintained in some cells by molecular chaperones expressed in other remote cells, using cell culture and *Drosophila* models of the polyglutamine diseases. Surprisingly, we found that exosome-mediated secretion and intercellular transmission of molecular chaperones are responsible for this non–cell-autonomous maintenance of proteostasis. Our study reveals novel insight into a

Significance

The heat shock response (HSR), a transcriptional response that up-regulates molecular chaperones upon heat shock, is known to be activated in a cell type-specific manner. Despite such imbalanced HSR upon stress, it is unclear as to how organismal protein homeostasis (proteostasis) is maintained. Here, we show that elevated expression of molecular chaperones in cells non-cell autonomously improves proteostasis in other cells. We further show that exosome-mediated secretion and intercellular transmission of chaperones are responsible for this non–cell-autonomous improvement of proteostasis. Our study reveals a molecular mechanism of non–cell-autonomous maintenance of organismal proteostasis that could functionally compensate for the imbalanced HSR among different cells, and also provides a novel physiological function of exosomes that contributes to maintenance of proteostasis.

Author contributions: T.T. and Y.N. designed research; T.T., M.S., N.F., H.A.P., and H.K. performed research; S.F. and K.W. contributed new reagents/analytic tools; T.T., M.S., N.F., and Y.N. analyzed data; T.T., H.A.P., and Y.N. wrote the paper; and S.F. and K.W. supervised the project.

The authors declare no conflict of interest.

This article is a PNAS Direct Submission.

[1]To whom correspondence should be addressed. Email: nagai@ncnp.go.jp.

This article contains supporting information online at www.pnas.org/lookup/suppl/doi:10.1073/pnas.1412651112/-/DCSupplemental.

molecular mechanism of non–cell-autonomous maintenance of proteostasis at the multicellular organismal level, which can functionally compensate for the imbalanced HSR among different cells and tissues under stressed conditions.

Results

Elevated Expression of HSPs in Cells Restores the Protein-Folding Environment in Other Cells. To examine whether cellular proteostasis is affected by the expression levels of chaperones in other cells, we set up an in vitro coculture experiment in which Neuro2A cells with different levels of chaperone expression were incubated separately across cell culture inserts (Fig. 1*A*). An expanded polyglutamine stretch of 81 repeats fused with EGFP (Q81-EGFP), a model aggregation-prone protein (15), readily forms insoluble aggregates as inclusion bodies in these cells, which can be easily visualized under the fluorescence microscope, and overexpression of HSPs has been reported to suppress such polyglutamine inclusions (16). We found that coculturing Q81-EGFP–expressing cells with cells overexpressing Hsp40 surprisingly resulted in less inclusion bodies (Fig. 1*C*), which was calculated as a 26% decrease in the number of inclusion bodies formed relative to the mock-transfected control cells (Fig. 1*D*). In addition, coincubation with the Hsp40-expressing cells resulted in improvement of cell viability of the Q81-EGFP–expressing cells (21% increase relative to the mock-transfected cells) (Fig. 1*E*). In contrast, coincubation with cells expressing Hsp40 mutants that are deficient for chaperone function [i.e., deletion mutants of Hsp40 that lack either the C-terminal and Gly/Phe-rich domains (Hsp40-J) or the N-terminal J domain (Hsp40-GC) (Fig. 1*B*)] showed no suppression of inclusion body formation (Fig. 1 *C* and *D*) or improvement of cell viability (Fig. 1*E*). These results indicate that elevated expression of Hsp40 in the cells leads to a non–cell-autonomous beneficial effect on the other cells, and that the chaperone activity of Hsp40 is responsible for this effect. Likewise, coculturing with Hsp70-expressing cells also decreased inclusion body formation (32% decrease) (Fig. 1 *F* and *G*) and improved cell viability (39% increase) (Fig. 1*H*) in the Q81-EGFP–expressing cells, whereas Hsp70 mutants lacking either ATPase activity [Hsp70(K71E)] (17) or substrate-binding activity (Hsp70dS) (Fig. 1*B*) had no such effects (Fig. 1 *F*–*H*). These results reveal that elevated levels of HSPs in a group of cells can improve the protein-folding environment and suppress polyglutamine-mediated cytotoxicity in another group of cells.

Hsp40 Is Secreted from Cells via a Nonclassical Pathway. Because the restoration of cellular proteostasis occurred without any physical contact between the two types of cells, we next asked whether extracellular factors released by the chaperone-expressing cells (i.e., activated signaling molecules or the overexpressed chaperones themselves) could be responsible for this non–cell-autonomous effect. We therefore focused our attention on the culture medium of Neuro2A cells in which Hsp40 was transiently transfected and investigated the responsible extracellular factors. To avoid contamination from dead cells, the culture medium was replaced with fresh medium at 24 h after transfection. Subsequent Western blot analysis of the culture medium revealed that Hsp40 itself was detected abundantly and accumulated over time in the culture medium (Fig. 2*A*), suggesting that cellular Hsp40 is released from cells into the extracellular space. Significant cell death was not detected by the lactate dehydrogenase release assay (Fig. S1*A*), which excludes the possibility of Hsp40 leakage from the dead cells under this condition. We further confirmed that endogenous Hsp40, as well as Hsc70 and Hsp90, is clearly detected in the culture medium, whereas the endoplasmic reticulum (ER)-resident chaperone Grp78

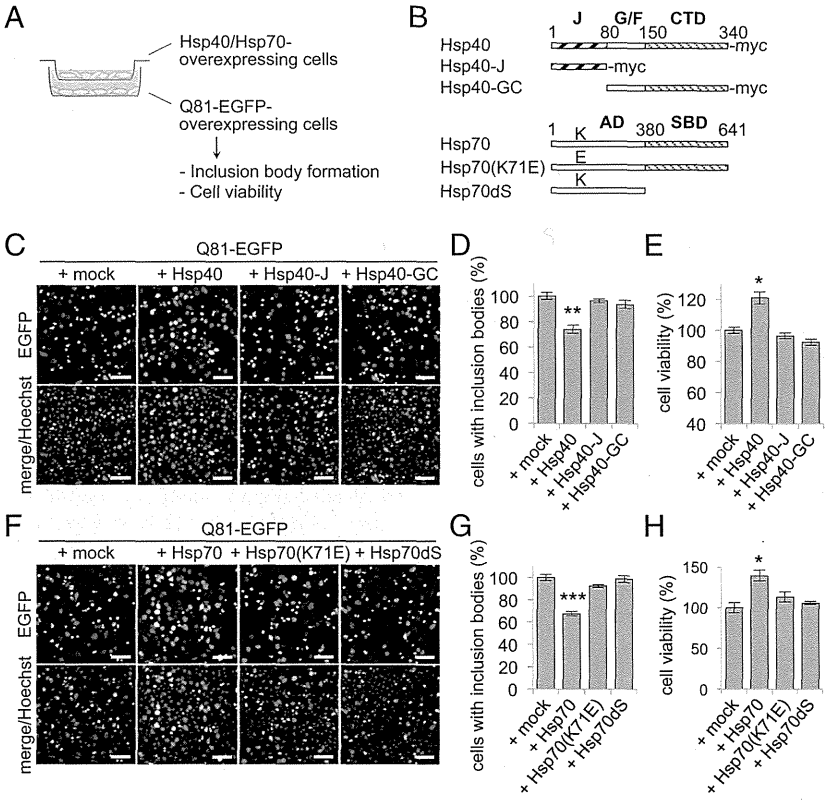

Fig. 1. Elevated expression of HSPs in cells restores the folding environment in other cells. (*A*) Schematic representation of the coculture experiment. Neuro2A cells expressing Q81-EGFP were coincubated with other Neuro2A cells overexpressing either Hsp40 or Hsp70 using a cell culture insert. (*B*) Hsp40, Hsp70, and their functionally deficient mutants used in this study. AD, ATPase domain; CTD, C-terminal domain; G/F, Gly/Phe-rich domain; J, J domain; SBD, substrate-binding domain. (*C* and *D*) Confocal microscopy images (*C*) and ratio of inclusion body formation (*D*) of Q81-EGFP–expressing cells that were cocultured with Hsp40-expressing cells for 20 h. (*E*) Cell viability of Q81-EGFP–expressing cells that were cocultured with Hsp40-expressing cells for 20 h. Incubation with the Hsp40-expressing cells significantly reduced inclusion body formation and increased survival rates in Q81-EGFP–expressing cells. (*F*–*H*) Inclusion body formation (*F* and *G*) and cell viability (*H*) of Q81-EGFP–expressing cells that were cocultured with Hsp70-expressing cells for 20 h. Data are represented as the mean ± SEM of three independent experiments (*$P < 0.05$, **$P < 0.01$, ***$P < 0.001$; Student's *t* test). Hoechst 33342 (Invitrogen) was used for nuclear staining in *C* and *F*. (Scale bars: *C* and *F*, 50 μm).

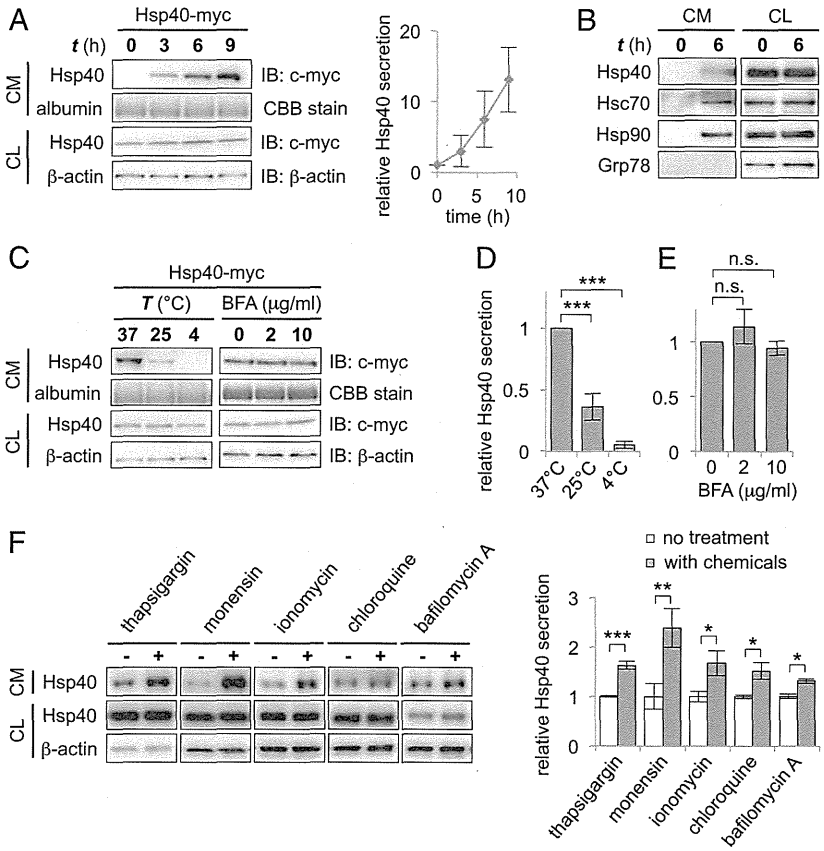

Fig. 2. Hsp40 is secreted from cells via a nonclassical pathway. (*A*) Western blotting analysis of culture media (CM) and cell lysates (CL) of Neuro2A cells that were transfected with myc-tagged Hsp40 (Hsp40-myc) (*Left*) and relative Hsp40 levels in the CM plotted against incubation time (*Right*). Serum albumin, which was stained by Coomassie Brilliant Blue (CBB), was used as a loading control for the CM. Hsp40 was detected abundantly and accumulated over time in the CM. IB, immunoblot. (*B*) Western blotting analysis of the CM and CL of nontransfected Neuro2A cells using antibodies against the indicated proteins. Endogenous Hsp40, Hsc70, and Hsp90 were detected in the CM of cells that were incubated 6 h after changing media, whereas the ER-resident Grp78 was not. (*C–E*) Western blotting analysis of the CM and CL of Hsp40-myc–expressing cells that were incubated for 6 h at different temperatures (*C*, *Left*) or that were treated with brefeldin A (BFA), an inhibitor of the classical secretion pathway (*C*, *Right*), and bar graphs demonstrating relative Hsp40 levels in the CM (*D* and *E*). Extracellular Hsp40 levels decreased at low temperatures but were not affected by BFA treatment, suggesting the involvement of a nonclassical pathway in the secretion of Hsp40. (*F*) Western blotting analysis showing the levels of endogenous Hsp40 in the CM and CL after 6 h of treatment with various chemicals that affect intracellular Ca^{2+} levels or endosomal transport (*Left*) and a bar graph showing relative Hsp40 levels in the CM (*Right*). Data are shown as the mean ± SEM of three independent experiments (*$P < 0.05$, **$P < 0.01$, ***$P < 0.001$; n.s., not significant; Student's *t* test). (Also Fig. S1.)

was not detected (Fig. 2*B*). Incubation of the cells at a low temperature, however, resulted in significant or almost complete suppression of Hsp40 release (64% and 95% decrease at 25 °C and 4 °C, respectively) compared with incubation at 37 °C (Fig. 2 *C* and *D*). These results reveal that Hsp40 is physiologically secreted from cells via a temperature-dependent cellular process, but not via cell death or passive diffusion across cell membranes.

Because Hsp40 is believed to be an intracellular protein, we then asked how Hsp40 gains access to the outside of cells. Most proteins targeted to the outside of cells have a signal sequence at their N terminus, which allows them to be secreted via the classical ER/Golgi pathway (18). However, Hsp40 lacks a distinct signal sequence for classical secretion, as analyzed by the signal peptide prediction program SignalP 4.1 (19). In agreement with this prediction, we found that Hsp40 secretion was insensitive to the treatment of cells with brefeldin A, an inhibitor of the ER/Golgi-dependent pathway (Fig. 2 *C* and *E*), whereas secretion of *Metridia* luciferase (MetLuc), a secretory protein containing an N-terminal signal peptide (18), was completely inhibited under the same condition (Fig. S1*B*). These results suggest that Hsp40 is secreted via a pathway that is different from the classical ER/Golgi-dependent pathway.

We then tested various chemical compounds that are reported to affect the nonclassical secretion pathways and examined their effects on the secretion levels of Hsp40. Treatment of Neuro2A cells with these compounds revealed that the chemicals that raise the intracellular Ca^{2+} level, such as thapsigargin, monensin, and ionomycin, significantly increased the secretion levels of endogenous Hsp40 (Fig. 2*F*). In addition, chloroquine and bafilomycin A, both of which perturb endosomal trafficking, affected Hsp40 secretion (Fig. 2*F*). Likewise, treatment of these chemicals resulted in an increase in secretion levels of other chaperones, including Hsp/Hsc70 and Hsp90 (Fig. S1*C*). These results strongly indicate that intracellular Ca^{2+} levels and endosomal transport act as key regulators of Hsp40 secretion.

Hsp40 Is Secreted via the Hsp/Hsc70-Dependent Exosome Pathway. Because both intracellular Ca^{2+} levels and endosomal transport have been suggested to be involved in the generation of exosomes (20), we decided to examine whether an exosome-mediated pathway could be involved in Hsp40 secretion. Following the established centrifugation protocol for the isolation of exosomes (21), we separated the supernatant (S100) and the pellet (P100) fractions from the culture medium of Neuro2A cells (Fig. 3*A*). We confirmed that the isolated P100 fraction contained small vesicles with uniformly rounded and cup-shaped morphology with a 50- to 100-nm diameter (Fig. 3*A*), which is in good agreement with the characteristics of exosomes (22). Western blotting of these fractions revealed that Hsp40 is indeed present in the P100 fraction, together with exosome-specific proteins, such as Alix, Flotillin-1, and GAPDH (23), but is not present in the S100 fraction (Fig. 3*B*). We further confirmed that Hsp40 is also detected in the P100 fractions from a broad range of cell lines, including SH-SY5Y, U373MG, C6, and mouse embryonic fibroblast (MEF) cells (Fig. 3*C*), and also in the P100 fraction purified from mouse serum (Fig. 3*D*). The P100 fraction was further analyzed by sucrose-density gradient centrifugation, showing that Hsp40 cofractionates with Hsc70 and Alix at a density of ~1.15 g/mL (Fig. 3*E*), which is consistent with the density of exosomes (1.13–1.19 g/mL) among various extracellular membrane vesicles (22). Immunoelectron microscopic analysis of this fraction revealed that Hsp40 is indeed detected inside the membrane vesicles (Fig. 3*F*). Furthermore, treatment of cells with GW4869, an exosome inhibitor (24), significantly suppressed the secretion of Hsp40, as

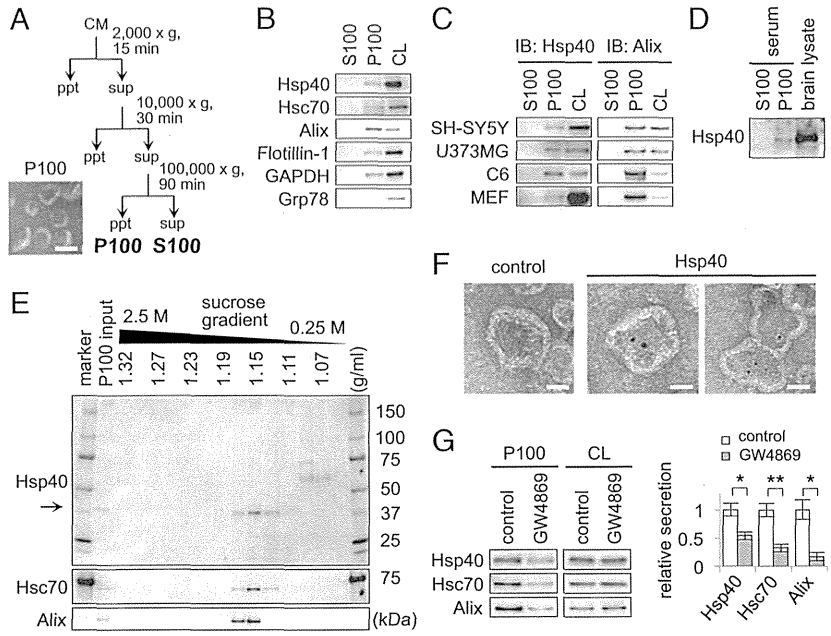

Fig. 3. Hsp40 is secreted via an exosome-mediated pathway. (*A*) Experimental scheme of the exosome purification. Sequential centrifugations of the CM eventually yield the supernatant (S100) and pellet (P100) fractions. (*Bottom Left*) EM image of the P100 fraction that was negatively stained with uranyl acetate. ppt, pellet; sup, supernatant. (Scale bar: 100 nm.) (*B*) Western blotting analysis of the S100 and P100 fractions obtained from the CM of Neuro2A cells using antibodies against the proteins indicated. Hsp40 was detected in the P100 fraction but not in the S100 fraction. (*C* and *D*) Western blotting analysis of the fractions obtained from the CM of SH-SY5Y, U373MG, C6, and WT MEF cells (*C*) and from the serum of 5-mo-old mice (*D*). (*E*) Western blotting analysis of the P100 fraction that was further separated by sucrose density gradient centrifugation with a sucrose gradient of 0.25–2.5 M. (*F*) Immunoelectron microscopic images of the P100 fraction that was stained with an Hsp40 antibody and a secondary antibody conjugated with 10-nm gold nanoparticles. For the control experiment, the P100 fraction was treated with the secondary antibody alone. (Scale bars: 50 nm.) (*G*) Western blotting analysis of the P100 fractions obtained from Neuro2A cells that were treated with the exosome inhibitor GW4869 (5 μM) for 6 h (*Left*) and a bar graph showing relative Hsp40 levels in the P100 fractions (*Right*). Data are shown as the mean ± SEM of three independent experiments (*$P < 0.05$, **$P < 0.01$; Student's *t* test).

well as the secretion of Hsc70 and Alix (Fig. 3*G*). Taken together, we conclude that Hsp40 is secreted via an exosome-mediated pathway.

We next examined the mechanism by which Hsp40 is secreted via the exosome pathway. To identify the domain within Hsp40 that is required for its secretion, we transfected plasmid vectors expressing deletion mutants of Hsp40 (Fig. 1*B*) and examined their secretion levels in the culture medium of Neuro2A cells. We found that Hsp40-J, which consists of the J domain alone, showed high levels of secretion, whereas Hsp40-GC, which lacks the J domain, was undetectable in the culture medium (Fig. 4*A*), suggesting an essential role of the J domain for Hsp40 secretion. To confirm this observation further, we designed an artificial chimeric protein, J-MetLucΔSP, in which the N-terminal signal peptide of the model secretory protein MetLuc was replaced with the Hsp40 J domain (Fig. 4*B*). Whereas the original MetLuc was detected in the S100 fraction (Fig. 4*C*) and its classical secretion was completely inhibited by treatment with brefeldin A (Fig. 4*D*, *Left*), we found that J-MetLucΔSP was detected in the P100 fraction (Fig. 4*C*) and its secretion was not affected by brefeldin A (Fig. 4*D*, *Right*). These results strongly suggest that domain swapping of the signal peptide to the J domain resulted in a pathway switch from classical to nonclassical secretion, confirming that the J domain is responsible for Hsp40 secretion via an exosome-mediated pathway. We also examined whether other Hsp40 family proteins that also have the highly conserved J domain (4) are secreted via an exosome-mediated pathway. Among those Hsp40 family proteins tested, the proteins that are localized in the cytosol, such as DnaJA1, DnaJA2, and DnaJB6a, were detected in the P100 fraction (Fig. 4*E*), whereas the proteins that are localized in the mitochondria (DnaJA3) or ER (DnaJC1) were not detected in either the P100 or S100 fraction (Fig. 4*E*). Thus, these results indicate that the cytosolic Hsp40s share the characteristic of exosomal secretion from cells.

Because the J domain acts as an interaction domain with Hsp/Hsc70 (4), we then examined whether Hsp/Hsc70 is involved in the exosome-mediated secretion of Hsp40. As expected, Hsc70 knockdown using RNAi resulted in significant suppression of Hsp40 secretion in the P100 fraction (51% decrease relative to control siRNA) (Fig. 4*F*), despite the increased cellular levels of Hsp40 that probably resulted from compensatory mechanisms in response to the decreased Hsc70 levels. This finding indicates that the exosomal secretion of Hsp40 is affected by the intracellular levels of Hsc70. In support of this finding, overexpression of Hsp70 resulted in a 122% increase in Hsp40 secretion relative to the mock-transfected cells (Fig. 4*G*). Thus, these results suggest that exosomal secretion of Hsp40 is regulated by Hsp/Hsc70 levels, probably by its interaction with Hsp/Hsc70 via its conserved J domain.

Exosomal Hsp40 Is Transmitted Intercellularly and Restores the Protein-Folding Environment in Recipient Cells. It has been reported that exosomes secreted from donor cells are internalized by recipient cells in an endocytosis-dependent manner (23). Accordingly, we either coincubated cells with the P100 fraction containing Hsp40-enhanced yellow fluorescent protein (EYFP) (Fig. 5 *A* and *B*) or cocultured them with other cells expressing Hsp40-EYFP (Fig. S2*A*), and found that Hsp40-EYFP fluorescent signals were clearly detected in the recipient cells, confirming that Hsp40 is also transmitted intercellularly using exosomes. Likewise, exosomal Hsp70 and Hsp90 are internalized by other cells (Fig. S2*B*). The transmitted HSPs in these experiments

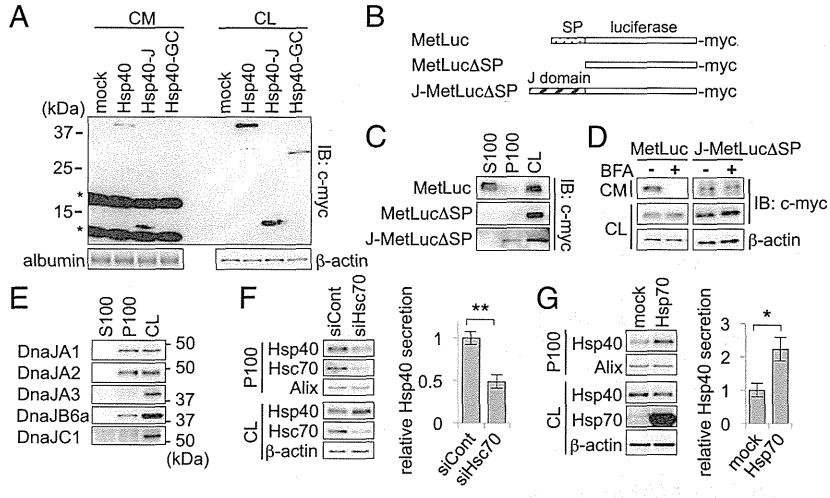

Fig. 4. Exosomal secretion of Hsp40 is dependent on the J domain and is regulated by Hsp/Hsc70. (*A*) Western blotting analysis of the CM and CL of Neuro2A cells expressing the Hsp40 deletion mutants. (*B*) Schematic representation of MetLuc and its mutants used in this experiment. SP, signal peptide. (*C*) Western blotting analysis of the fractions obtained from the CM of cells expressing the MetLuc mutants. The mutant J-MetLucΔSP, which contains a J domain instead of a secretory SP, was detected in the P100 fraction, whereas the original MetLuc was detected in the S100 fraction. (*D*) Western blotting analysis showing the extracellular secretion levels of the MetLuc mutants after treatment with BFA (10 μg/mL). (*E*) Western blotting analysis of the P100 fractions separated from the CM of Neuro2A cells using antibodies against various Hsp40 family proteins. The cytosolic family proteins of Hsp40, including DnaJA1, DnaJA2, and DnaJB6a, were detected in the P100 fraction, whereas mitochondrial DnaJA3 and ER-resident DnaJC1 were not. (*F* and *G*) Western blotting analysis of the P100 fractions obtained from cells transfected with an Hsc70 siRNA (*F*, *Left*) or an Hsp70-encoding plasmid (*G*, *Left*) and bar graphs showing relative levels of Hsp40 secretion (*F*, *Right* and *G*, *Right*, respectively). siCont, small interfering RNA for negative control. Data are shown as the mean ± SEM of three independent experiments (*$P < 0.05$, **$P < 0.01$; Student's *t* test).

showed almost identical punctate fluorescent patterns that were distributed around the nucleus, which are in good agreement with the endocytosis-mediated internalization of exosomes. Because exosomes are known to deliver various biomolecules transcellularly, such as mRNAs, microRNAs, and proteins, which function to exert their bioactivities in recipient cells after their internalization (25, 26), we hypothesized that Hsp40 transmitted intercellularly in an exosome-dependent manner also exerts its function as a molecular chaperone in recipient cells to restore the protein-folding environment.

To test this hypothesis, exosomes purified from the culture medium of donor cells were added to recipient cells expressing polyglutamine protein, and aggregation was analyzed (Fig. 5*A*). Incubation of the P100 fraction purified from Hsp40-expressing donor cells significantly suppressed inclusion body formation in the Q81-EGFP–expressing recipient cells (Fig. 5*C*), resulting in a 57% decrease in the number of inclusions relative to the untreated control recipient cells (Fig. 5*D*). The filter trap assay confirmed that insoluble aggregates in the Q81-EGFP–expressing cells were effectively reduced by treatment with the P100 fraction derived from the Hsp40-expressing cells (Fig. 5*E*). The P100 fraction purified from the Hsp70-expressing cells also showed similar suppressive effects (Fig. S3 *A* and *B*). These results suggest that extracellularly added exosomes that are secreted from the chaperone-expressing donor cells improve the protein-folding environment in the recipient cells. It is noted that the P100 fraction, but not the S100 fraction, suppressed Q81-EGFP aggregation (Fig. S3 *C* and *D*) in a dose-dependent manner (Fig. S3*E*), indicating that the suppressive effects may be due to endogenous molecules within the exosomes. Because the amount of Hsp40 secreted in the P100 fraction was significantly increased by overexpression of Hsp40 in the donor cells (Fig. S3*F*, *Left*), which resulted in enhanced suppressive effects in the recipient cells (Fig. 5 *C*–*E*), the Hsp40 that is transmitted by exosomes should be one of the factors responsible for these effects. In support of this idea, the P100 fraction with a lower level of Hsp40, which was purified from donor cells transfected with an Hsp40-specific siRNA (Fig. S3*F*, *Right*), showed less ability to suppress inclusion body formation (Fig. 5 *F* and *G*) and to reduce the insoluble aggregates of Q81-EGFP (Fig. 5*H*) than the P100 fraction from the control siRNA-transfected cells. Thus, these results indicate that exosome-mediated intercellular transmission of Hsp40 restores the cellular protein-folding environment in a non–cell-autonomous manner.

Exosome-Mediated Intercellular Transmission of HSPs Is Activated Under Stressed Conditions and Compensates for the Protein-Folding Environment in HSR-Deficient Cells. When challenged by proteotoxic stresses, cells transiently activate the HSR, which is a cell-autonomous mechanism to maintain cellular proteostasis. Therefore, we next asked whether the exosome-mediated non–cell-autonomous mechanism that improves the protein-folding environment in surrounding cells could also be activated under stressed conditions. Cells were heat-shocked at 42 °C, and the contents of the exosomes produced by these cells were examined as above. We found that heat stress indeed resulted in an increase in the levels of HSPs, including Hsp40, Hsp70, and Hsp90, not only in the cytosol but also in the P100 fraction from the Neuro2A cells (Fig. 5*I*). Addition of the P100 fraction purified from the heat-shocked donor cells resulted in more effective suppression of inclusion body formation in the Q81-EGFP–expressing recipient cells compared with the P100 fraction from the unstressed cells (Fig. 5 *J* and *K*). These results indicate that, under stressed conditions, not only the expression of intracellular HSPs but also the exosome-mediated intercellular transmission of HSPs is activated to non-cell autonomously improve the cellular protein-folding environment.

The above findings led us to hypothesize that cells with only limited levels of chaperone induction even under stressed conditions might be protected by the exosome-mediated transmission of HSPs from other chaperone-expressing cells. To test this hypothesis, we used HSF1-null MEF cells, an HSR-deficient cell line that lacks the heat shock-mediated induction

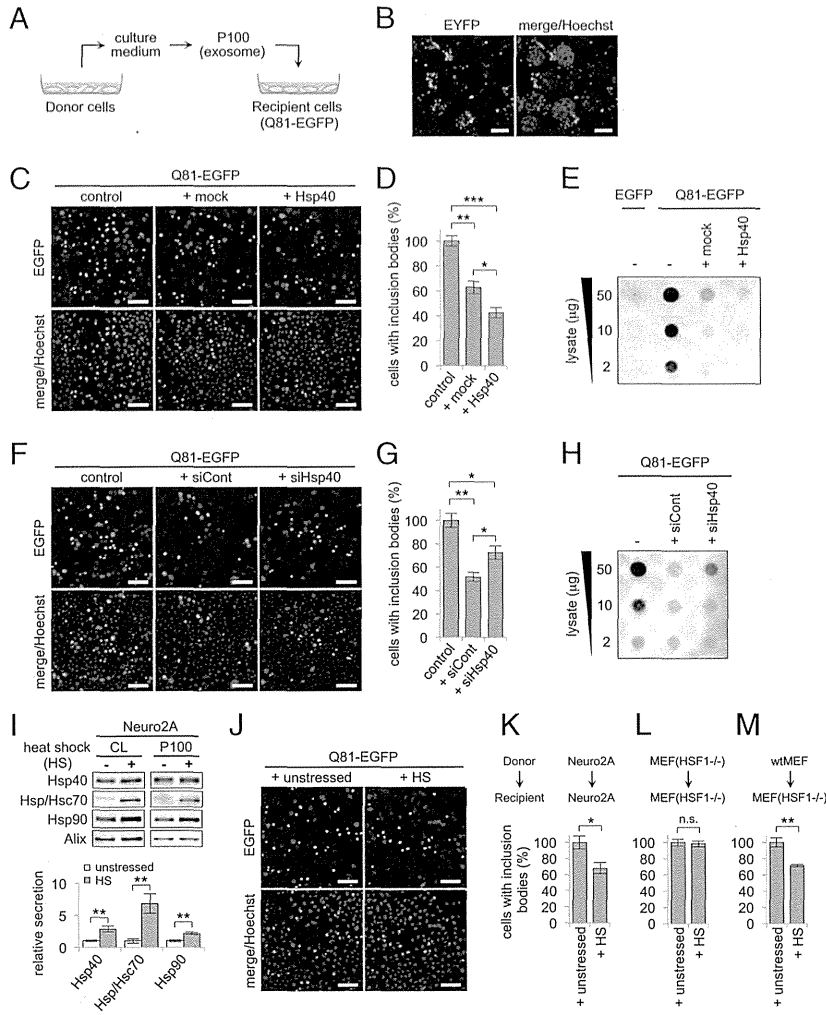

Fig. 5. Exosomal Hsp40 is transmitted intercellularly and restores the protein-folding environment in recipient cells. (*A*) Schematic representation of the exosome-transfer experiment. P100 fractions were purified from the culture medium of donor Neuro2A cells and added to the culture medium of recipient Neuro2A cells that were overexpressing Q81-EGFP. (*B*) Confocal microscopy images of Neuro2A cells that were incubated with the P100 fraction obtained from Hsp40-EYFP–expressing cells. (*C* and *D*) Confocal microscopy images (*C*) and a bar graph showing the ratio of inclusion body formation (*D*) of Q81-EGFP–expressing recipient cells that were incubated with the P100 fraction obtained from the mock- or Hsp40-transfected donor cells. (*E*) Filter trap assay of Q81-EGFP–expressing cells that were incubated with the P100 fraction obtained from the mock- or Hsp40-transfected cells. Incubation with the P100 fraction from the Hsp40-expressing cells resulted in a significant reduction in the number of inclusion bodies (*D*) and in the amount of insoluble aggregates (*E*) formed in the recipient Q81-EGFP–expressing cells compared with the untreated control cells. (*F–H*) Inclusion body formation (*F* and *G*) and filter trap assay (*H*) of Q81-EGFP–expressing cells that were incubated with the P100 fractions from cells transfected with the control siRNA or Hsp40 siRNA. (*I*) Western blotting analysis (*Top*) and a bar graph (*Bottom*) of P100 fractions that were separated from the heat-shocked Neuro2A cells. Heat shock (HS) resulted in an increase in the secretion of HSPs via exosomes. (*J* and *K*) Confocal microscopy images (*J*) and a bar graph showing the ratio of inclusion body formation (*K*) of Q81-EGFP–expressing Neuro2A cells that were incubated with the P100 fraction isolated from the unstressed or heat-shocked Neuro2A cells at 42 °C for 30 min. (*L* and *M*) Bar graphs showing the ratio of inclusion body formation of Q81-EGFP–expressing recipient HSF1-null MEF cells that were incubated with the P100 fractions isolated from the heat-shocked donor HSF1-null MEF cells (*L*) or the heat-shocked donor WT MEF cells (*M*). Data are represented as the mean ± SEM of three independent experiments (**P* < 0.05, ***P* < 0.01, ****P* < 0.001; Student's *t* test). Hoechst 33342 was used for nuclear staining in *B*, *C*, *F*, and *J*. (Scale bars: *B*, 10 μm; *C*, *F*, and *J*, 50 μm.) (Also Figs. S2 and S3.)

of HSPs (27), and repeated the above experiments. In contrast to Neuro2A cells, incubation of HSF1-null MEF cells at 42 °C resulted in no significant increase in the expression levels of HSPs or their secretion levels in the P100 fraction (Fig. S3*G*). As expected, addition of the P100 fraction purified from the heat-shocked HSF1-null MEF cells resulted in no enhancement of the suppressive effects on Q81-EGFP aggregation in the recipient HSF1-null MEF cells compared with the P100 fraction from the unstressed cells (Fig. 5*L* and Fig. S3*H*). These results indicate that HSR-deficient cells lack not only the cell-autonomous HSR but also the exosome-mediated intercellular protective response against proteotoxic stresses, both of which may contribute to their vulnerability to stress. However, the extracellular addition of the P100 fraction purified from the heat-shocked WT MEF cells resulted in efficient suppression of inclusion body formation even in the Q81-EGFP–expressing HSF1-null MEF cells (Fig. 5*M* and Fig. S3*I*), suggesting that the lack of the protective responses in HSR-deficient cells could be functionally compensated for by exosomes secreted from other HSR-inducible cells. Thus, these results indicate that the proteostasis in cells that lack

the cell-autonomous HSR could be non-cell autonomously maintained by the surrounding chaperone-expressing cells, via the enhanced exosomal release and intercellular transmission of HSPs.

Elevated Expression of HSPs Non-Cell Autonomously Suppresses Polyglutamine-Mediated Neurodegeneration in Remote Tissues in Vivo. We next asked whether this non–cell-autonomous restoration of proteostasis is also conserved at the multicellular organismal level in vivo. We used *Drosophila melanogaster* models, in which the conditional expression of transgenes in a tissue-specific manner can be easily achieved using the Gal4-upstream activation sequence (UAS) system. To monitor the non–cell-autonomous effect of HSPs, flies conditionally expressing HSPs under the control of various tissue-specific Gal4 drivers were crossed with GMR-HttQ120 flies, a polyglutamine disease model fly line that constitutively expresses a mutant huntingtin protein with 120 polyglutamine repeats, under the compound eye-specific GMR promoter (28). We then examined whether progression of polyglutamine-mediated degeneration in photoreceptor neurons could be affected by the elevated expression of HSPs in other tissues.

In the control GMR-HttQ120 flies, the compound eyes progressively degenerated due to expression of the polyglutamine protein (Fig. 6*A*, *i–iv*) (28). Increased expression of Hsp40 in the same tissue using the GMR-Gal4 driver resulted in cell-autonomous suppression of photoreceptor degeneration (Fig. 6*D*, *vi*) compared with the control flies expressing GFP (Fig. 6*D*, *ii*), as reported previously (29). Surprisingly, Hsp40 overexpression in the pigment cells, which are located next to the photoreceptor neurons, using the 54C-Gal4 driver (30) also resulted in morphological improvement of photoreceptor degeneration during the 7–21 d after eclosion (Fig. 6*A*, *vi–viii*). Upon quantitative evaluation by counting the number of remaining rhabdomeres in each ommatidium, we found that elevated expression of Hsp40 in the pigment cells resulted in a significant increase in the number of rhabdomeres per ommatidium, calculated as 64%, 66%, and 45% rescue in the GMR-HttQ120 flies at 7, 14, and 21 d of age relative to the GFP-expressing control flies, respectively (Fig. 6*B*). Consistently, Hsp40 expression using another pigment cell-specific driver, rdhB-Gal4, also ameliorated the photoreceptor degeneration in the GMR-HttQ120 flies (Fig. 6*E* and Fig. S4*A*, *vi* vs. *ii*). These results indicate that pigment cell-specific expression of Hsp40 non-cell autonomously suppresses the degeneration of photoreceptor neurons in neurotoxic HttQ120-expressing flies. Similarly, Hsp70 expression in the pigment cells also resulted in non–cell-autonomous suppression of photoreceptor degeneration in these flies (Fig. 6*B* and Fig. S4*B*). In contrast, GMR-HttQ120 flies bearing the UAS-Hsp40/Hsp70 transgenes, but not the pigment cell-specific Gal4 drivers, showed no improvement in rhabdomere number or photoreceptor degeneration (Fig. 6*C* and Fig. S4*C*), suggesting that possible leak expression of these chaperones from the UAS-Hsp40/Hsp70 transgenes is at a negligible level in this study. These data suggest that the increased level of Hsp40/Hsp70 in the pigment cells leads to non–cell-autonomous suppression of polyglutamine-dependent degeneration in the neighboring photoreceptor neurons in vivo, although we cannot exclude the possibility that the rescue of photoreceptor degeneration may be attributed to the improved appearance of the overall structures of the eyes by pigment-specific expression of HSPs.

To exclude such a possibility, we next examined whether non–cell-autonomous restoration of proteostasis is maintained between not only adjacent tissues but also physically remote tissues. We therefore generated GMR-HttQ120 flies with elevated Hsp40 expression in remote tissues, such as muscle and fat body. The expression patterns of the tissue-specific Gal4 drivers used in this experiment were confirmed using GFP as a reporter

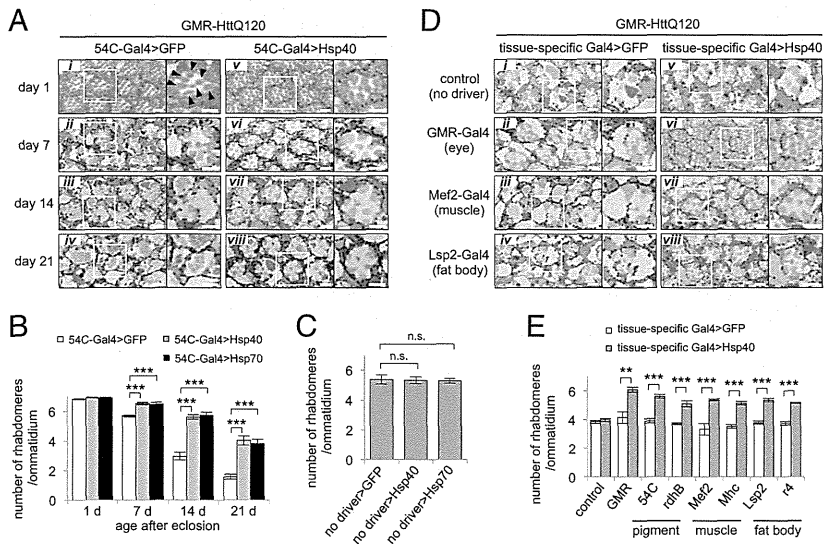

Fig. 6. Elevated expression of HSPs non-cell autonomously suppresses polyglutamine-mediated neurodegeneration in remote tissues in vivo. (*A*) Microscopic images of compound eye sections of adult GMR-HttQ120 flies expressing GFP or Hsp40 in pigment cells at 1–21 d of age. (*Right*) Magnified images of a representative ommatidium. (*i*) Rhabdomeres are indicated by arrowheads. Whereas control GFP flies (*i–iv*) showed progressive eye degeneration due to the expression of toxic polyglutamine proteins in photoreceptor neurons, flies coexpressing Hsp40 in the pigment cells (*v–viii*) showed significant morphological improvement of neurodegeneration. (*B*) Average number of rhabdomeres per ommatidium in GMR-HttQ120 flies expressing GFP, Hsp40 (*A*) or Hsp70 (Fig. S4*B*) in the pigment cells. GMR-HttQ120 flies expressing either Hsp40 or Hsp70 in the pigment cells showed a greater number of surviving rhabdomeres than control flies between day 7 and day 21. (C) Number of rhabdomeres per ommatidium in GMR-HttQ120 flies without the pigment cell-specific Gal4 driver at 7 d of age (Fig. S4C). (*D*) Microscopic images of compound eye sections of GMR-HttQ120 flies at 11 d of age that were coexpressing GFP (*ii–iv*) or Hsp40 (*vi–viii*) in specific tissues, including compound eyes (GMR-Gal4, *ii* and *vi*), muscle (Mef2-Gal4, *iii* and *vii*), and fat body (Lsp2-Gal4, *iv* and *viii*). (*i* and *v*) As a negative control, GMR-HttQ120 flies without tissue-specific Gal4 drivers are shown. (*E*) Number of rhabdomeres per ommatidium calculated from *D* and from Fig. S4*A*. Data are represented as the mean ± SEM of at least five flies (***P* < 0.01, ****P* < 0.001; Student's *t* test). (Scale bars: *A* and *D*, 5 μm.) (Also Figs. S4 and S6.)

(Fig. S5*A*). Surprisingly, muscle-specific expression of Hsp40 using either the Mef2-Gal4 or Mhc-Gal4 driver resulted in effective suppression of photoreceptor degeneration in the GMR-HttQ120 flies (Fig. 6*D*, *vii* vs. *iii* and Fig. S4*A*, *vii* vs. *iii*), calculated as 56% or 47% rescue in the number of rhabdomeres, respectively (Fig. 6*E*). Similarly, fat body-specific expression of Hsp40 using either the Lsp2-Gal4 or r4-Gal4 driver also improved photoreceptor degeneration (49% and 43% rescue, respectively) (Fig. 6 *D*, *viii* vs. *iv* and *E* and Fig. S4*A*, *viii* vs. *iv*). Moreover, tissue-specific expression of Hsp70 in muscle and fat body also ameliorated the photoreceptor degeneration in the GMR-HttQ120 flies, whereas expression of a deficient mutant of Hsp70 lacking a substrate-binding domain (Hsp70dS) did not show such beneficial effects under the same condition (Fig. S6 *A* and *B*). The leak expression of UAS transgenes was excluded by immunohistochemistry and quantitative RT-PCR analyses using GFP as a reporter, showing that no GFP expression was detected in the compound eyes of the UAS-GFP flies bearing the Mef2-Gal4 or Lsp2-Gal4 driver (Fig. S5 *B* and *C*). Thus, these results reveal that elevated levels of HSPs in one tissue can non-cell autonomously suppress polyglutamine-mediated degeneration in another remote tissue without any direct cell-to-cell contact.

Non–Cell-Autonomous Suppression of Polyglutamine-Mediated Neurodegeneration by Hsp40 Occurs via Ykt6-Dependent Exosomal Secretion. We then asked whether exosomal secretion from Hsp40-expressing tissues is responsible for the non–cell-autonomous restoration of proteostasis observed in our *Drosophila* models. Ykt6, which is one of the R-SNARE proteins, has been reported to be necessary for exosome secretion in *Drosophila*, because depletion of this protein caused the accumulation of exosome proteins inside cells, resulting in a corresponding decrease in the extracellular levels of those proteins (31). Therefore, we reduced the level of Ykt6 in the Hsp40-expressing tissues by RNAi-mediated knockdown and examined its effect on polyglutamine-mediated degeneration in photoreceptor neurons in the GMR-HttQ120 flies, as above.

The GMR-HttQ120 flies coexpressing Hsp40 and an inverted repeat RNA (IR) against Ykt6 in pigment cells under the rdhB-Gal4 driver showed a similar level of severe photoreceptor degeneration to the control GMR-HttQ120 flies coexpressing GFP (Fig. 7*A*, *iv* vs. *iii*), demonstrating that Ykt6 knockdown almost completely cancels the non–cell-autonomous improvement observed in the Hsp40-expressing GMR-HttQ120 flies without Ykt6 knockdown (Fig. 7*A*, *ii* vs. *i*). Quantitative analyses revealed that GMR-HttQ120 flies with pigment-specific expression of Hsp40 and Ykt6 knockdown failed to show a significant increase in the number of rhabdomeres per ommatidium relative to the corresponding GFP-expressing GMR-HttQ120 flies, whereas significant rescue (42%) was observed in the Hsp40-expressing GMR-HttQ120 flies without Ykt6 knockdown (Fig. 7*B*, *Left*). Expression of the Ykt6 IR using the rdhB-Gal4 driver had no significant effects on photoreceptor degeneration in the control GFP-expressing GMR-HttQ120 flies (Fig. 7 *A*, *iii* vs. *i* and *B*, *Left*), suggesting that pigment-specific knockdown of Ykt6 itself has no deleterious effects in photoreceptor neurons. These results indicate that Ykt6 expression in the Hsp40-expressing tissues plays a critical role in the non–cell-autonomous improvement of photoreceptor degeneration in the GMR-HttQ120 flies. Consistent with this finding, Ykt6 knockdown in the fat body using the Lsp2-Gal4 driver in the Hsp40-expressing GMR-HttQ120 flies also largely cancelled the non–cell-autonomous improvement of photoreceptor degeneration (Fig. 7*A*, *v–viii*), whereas 49% rescue was observed in the corresponding Hsp40-expressing GMR-HttQ120 flies without Ykt6 knockdown (Fig. 7*B*, *Right*). Thus, we conclude that non–cell-autonomous suppression of polyglutamine-mediated neurodegeneration by remote tissue-specific expression of Hsp40 in *Drosophila* depends on Ykt6-mediated exosomal secretion.

Discussion

In this study, we demonstrated that elevated expression of HSPs, such as Hsp40 and Hsp70, in specific cells and/or tissues leads to the suppression of polyglutamine-mediated proteotoxicity in other remote cells and/or tissues, both in cultured cells and in *Drosophila*. We further provide definite evidence that this non–cell-autonomous beneficial effect is mediated by exosomes, one of the extracellular membrane vesicles secreted from cells, by which HSPs are transmitted intercellularly and improve the protein-folding environment in the recipient cells. Our observations are compatible with previous reports showing non–cell-autonomous effects of molecular chaperones in polyglutamine disease mice models and *Caenorhabditis elegans* (32), although

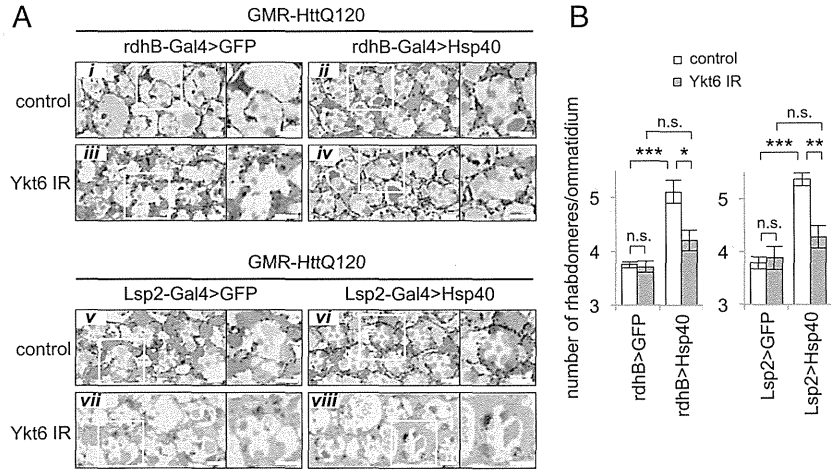

Fig. 7. Non–cell-autonomous suppression of polyglutamine-mediated neurodegeneration by Hsp40 occurs via Ykt6-dependent exosomal secretion. (*A*) Microscopic images of compound eye sections of GMR-HttQ120 flies coexpressing both Hsp40 and Ykt6 IR in pigment cells using rdhB-Gal4 (*Top*) or in fat body using Lsp2-Gal4 (*Bottom*). Ykt6 knockdown cancelled the morphological improvement of photoreceptor degeneration of GMR-HttQ120 flies expressing Hsp40 in either pigment cells or fat body. (Scale bars: *A*, 5 μm.) (*B*) Number of rhabdomeres per ommatidium in GMR-HttQ120 flies expressing both Hsp40 and Ykt6 IR in pigment cells (rdhB-Gal4, *Left*) or in fat body (Lsp2-Gal4, *Right*). Data are represented as the mean ± SEM of at least five flies (**P* < 0.05, ***P* < 0.01, ****P* < 0.001; Student's *t* test).

their molecular bases remained unclear. Thus, the present study is the first report, to our knowledge, to reveal the molecular mechanism for the non–cell-autonomous maintenance of organismal proteostasis that relies on cell-to-cell communication of HSPs using exosomes.

We propose the following model for the mechanism by which multicellular organisms maintain their global proteostasis under stressed conditions, despite the imbalanced transcriptional responses of chaperone expression among different cells (Fig. S7). Upon exposure to stresses, some cells activate the HSR to protect themselves from the proteotoxic consequences, whereas some cells do not, resulting in a cell- and/or tissue-specific imbalance in the expression levels of HSPs in multicellular organisms (9–11). Although the biological significance of the imbalanced transcriptional responses remains to be elucidated at the present stage, this chaperone imbalance is functionally compensated for by the intercellular transmission of HSPs via exosomes. We showed that proteotoxic challenges, such as heat stress, activate the exosome-mediated secretion of HSPs (Fig. 5*I*), which transcellularly increases the proteostasis capacity not only of the WT recipient cells (Fig. 5 *J* and *K*) but also of the HSF1-null recipient cells, an HSR-deficient cell line lacking HSF1-mediated up-regulation of molecular chaperones (Fig. 5*M* and Fig. S3*I*). Our results indicate that exosome-mediated regulation of proteostasis does not require HSF1 in the recipient cells, and thus is capable of compensating the imbalanced activity of the HSR among different cells without the involvement of transcription. In this regard, the compensatory mechanism presented in this study is distinct from the neuronal control of HSF1 activity in peripheral tissues in *C. elegans* (33). We speculate that multicellular organisms have developed an integrated protective system against cellular stresses consisting of the cell-autonomous HSR and the exosome-mediated transmission of HSPs, both of which complementarily serve as a global stress response to maintain organismal proteostasis.

It has been reported that HSPs, such as Hsp27, Hsp70, and Hsp90, are secreted from cells and that this process is significantly activated by heat stress and physical stress, including exercise (34–36). However, the physiological roles of the extracellular HSPs have remained poorly understood, except for the immunological function of Hsp70, which stimulates cytokine production in monocytes (37). In this study, we clearly demonstrate that the secreted Hsp40 is transmitted intercellularly via exosomes, which improves the protein-folding environment in the other cells. This observation is quite reasonable because it is unlikely that Hsp40, a cochaperone of Hsp70 that requires ATP for its function, would exert chaperoning activity in the extracellular space where ATP does not exist; rather, the secreted Hsp40 moves back to the intracellular environment where ATP is supplied so that it can function as a molecular chaperone. In agreement with our findings, the glia-to-neuron transmission of proteins, including heat shock-induced proteins, has been suggested, which may protect neurons from acute injury or stress (38, 39). Our results indicate that the maintenance of organismal proteostasis by exosome-mediated transmission is a previously unidentified role of the extracellular HSPs.

Exosomes are reported to mediate the intercellular transmission of their cargo molecules, thereby facilitating the non–cell-autonomous control of various physiological functions: for example, the transfer of RNAs that regulate the expression of specific target genes (25) or can be translated into proteins (26) and the stimulation of adaptive immune responses that can enhance antitumor activity (40). Here, we reveal a novel physiological function of exosomes, namely, the transmission of molecular chaperones among different cells that contributes to the maintenance of organismal proteostasis. Interestingly, proteins bearing a J domain, such as cytosolic Hsp40 families and the artificial chimeric protein J-MetLucΔSP, are secreted via exosomes, and Hsp40 secretion highly depends on the cellular levels of Hsp/Hsc70 (Fig. 4). These findings indicate that the J domain serves as a sorting tag for Hsp/Hsc70 to load the cytosolic J proteins selectively into exosomes, although how Hsp/Hsc70 is sorted into exosomes is unknown. Recently, sumoylation of hnRNPA2B1 has been reported to regulate the sorting of microRNAs into exosomes through binding to their short-sequence motifs (41). Taken together, J domain-dependent loading of J proteins by Hsp/Hsc70 could be one of the sorting mechanisms by which different cellular proteins and nucleic acids can be specifically sorted into individual exosomes, which may determine and regulate the diverse functions of exosomes.

Accumulation of misfolded proteins is a characteristic of several neurodegenerative diseases; thus, the induction of molecular chaperones has been suggested as a therapeutic strategy for such diseases (8). We showed that polyglutamine-mediated photoreceptor degeneration in *Drosophila* is suppressed by the increased expression of HSPs not only in the same tissues but also in other remote tissues (Fig. 6), and that this non–cell-autonomous effect is canceled by the disruption of Ykt6-mediated exosome secretion (Fig. 7). We further demonstrated that the secretion levels of HSPs via exosomes correspond well to their expression levels in the cytosol in cell culture (Fig. S3*F*). Furthermore, heat shock has been reported to enhance the exosomal release of HSPs highly (42). These findings suggest that the induction of HSPs in one tissue increases the secretion of HSPs via exosomes, which facilitates the exosome-mediated transmission of HSPs among different cells and improves proteostasis in other remote tissues. Thus, we propose that the enhancement of the exosomal secretion of HSPs, as well as the activation of the cell-autonomous HSR, is a potential therapeutic strategy for the protein-misfolding diseases.

Materials and Methods

Purification of Exosomes. Exosomes were prepared as described previously (21). Briefly, the culture medium of cells harvested in a 100-mm dish was replaced with exosome-depleted medium in which serum-derived exosomes were removed by ultracentrifugation at 100,000 × *g* for 16 h. After 24-h incubation, culture supernatants were collected and centrifuged sequentially at 2,000 × *g* for 15 min, 10,000 × *g* for 30 min, and 100,000 × *g* for 120 min. The pellet (P100) containing exosomes was resuspended in appropriate buffers. All centrifugations were performed at 4 °C.

Analysis of Inclusion Body Formation of Polyglutamine Proteins. Cells were transfected with a Q81-EGFP–encoding plasmid vector using Lipofectamine LTX and PLUS reagent (Invitrogen) and incubated for 4 h. The medium was then replaced with fresh medium with or without P100 fractions. The cells were further incubated for 20 h and then subjected to microscopic analysis using a confocal microscope (FV1000; Olympus). Inclusion body formation was calculated as the ratio of the number of cells with inclusion bodies to the total number of transfected cells. For each sample, 700–1,300 transfected cells were analyzed, and the experiments were independently repeated at least three times.

EM. Membrane vesicles, including exosomes, were prepared as described above. Vesicles were deposited on collodion-carbon–coated grids and fixed with 2% (wt/vol) paraformaldehyde. For immunoelectron microscopy, the vesicles were permeabilized with 0.1% saponin, followed by immunolabeling with an anti-Hsp40 (DnaJB1) antibody (Stressgen) and a secondary antibody conjugated with 10-nm gold particles (Sigma). The vesicles were negatively stained with uranyl acetate and analyzed with a transmission electron microscope (Tecnai Spirit; FEI).

Fly Stocks. Flies were cultured and crossed under standard conditions at 25 °C. The transgenic fly lines bearing the GMR-HttQ120, UAS-GFP, UAS-Hsp70, UAS-Ykt6 IR, or tissue-specific GAL4 (GMR, 54C, rdhB, Mef2, Mhc, Lsp2, and r4) transgene were obtained from the Bloomington Drosophila Stock Center. For the generation of a transgenic fly line bearing the UAS-Hsp40 transgene, a DNA fragment coding for *Drosophila* Hsp40 (DnaJB1) was amplified from pOT2 cDNA clone GH26396 (obtained from the Drosophila Genetic Resource Center, Kyoto Institute of Technology) by PCR and was inserted into the pUAST vector. The resultant vector was injected into fly embryos by standard procedures to establish Hsp40 fly lines.

Histology. Preparation of fly thin sections and evaluation of photoreceptor degeneration were performed as previously reported (43). Briefly, heads of GMR-HttQ120 flies were fixed in 2% paraformamide and 2.5% (wt/vol) glutaraldehyde and embedded in Epon. Compound eyes were then sectioned at 1 μm and stained with 1% toluidine blue. Microscopic images were obtained using a BX51 microscope with a DP71 CCD camera (Olympus), and the average number of rhabdomeres in each ommatidium was calculated. In all cases, the number of rhabdomeres was counted in 16 ommatidia in each section and at least six different sections from each eye were analyzed and averaged. The data are shown as the mean ± SEM of five to eight flies. The values of "% rescue" were calculated as follows:

$$\%\ \text{rescue} = (I_{HSP} - I_{GFP}) \times 100/(I_{total} - I_{GFP}),$$

in which I_{HSP} and I_{GFP} are the numbers of rhabdomeres per ommatidium in flies expressing HSPs and GFP, respectively, and I_{total} is the total number of rhabdomeres per ommatidium ($I_{total} = 7$).

ACKNOWLEDGMENTS. We thank Drs. Kenzo Otsuka (Chubu University), Akira Nakai (Yamaguchi University), and Hideaki Itoh (Akita University) and Soh Yamamoto (Sapporo Medical University) for kindly providing the Hsp40 cDNA (DnaJB1), HSF1-null MEF cells, and Hsp90 cDNA, respectively. We also thank Yoshiko Hara and Tomoko Okada for their technical assistance. This work was supported, in part, by Grants-in-Aid for Scientific Research on Priority Areas (Research on Pathomechanisms of Brain Disorders, Protein Community, and Proteolysis to Y.N.) and on Innovative Areas (Synapse and Neurocircuit Pathology to Y.N.) from the Ministry of Education, Culture, Sports, Science, and Technology, Japan; by Grants-in-Aid for Scientific Research (B; to Y.N.) and for Japan Society for the Promotion of Science (JSPS) Fellows (to T.T.) and for Young Scientists (A; to T.T.) from the JSPS, Japan; by Health Labor Sciences Research Grants for Research on Development of New Drugs, Research on Intractable Diseases, and the Research Committee for Ataxic Diseases (to Y.N.) from the Ministry of Health, Labor, and Welfare, Japan; by a grant from Core Research for Evolutional Science and Technology of the Japan Science and Technology Agency (to Y.N.); and by a grant from the Asahi Glass Foundation (to T.T.).

1. Hartl FU, Bracher A, Hayer-Hartl M (2011) Molecular chaperones in protein folding and proteostasis. *Nature* 475(7356):324–332.
2. Akerfelt M, Morimoto RI, Sistonen L (2010) Heat shock factors: Integrators of cell stress, development and lifespan. *Nat Rev Mol Cell Biol* 11(8):545–555.
3. Bukau B, Weissman J, Horwich A (2006) Molecular chaperones and protein quality control. *Cell* 125(3):443–451.
4. Kampinga HH, Craig EA (2010) The HSP70 chaperone machinery: J proteins as drivers of functional specificity. *Nat Rev Mol Cell Biol* 11(8):579–592.
5. Carrell RW, Lomas DA (1997) Conformational disease. *Lancet* 350(9071):134–138.
6. Soto C, Estrada LD (2008) Protein misfolding and neurodegeneration. *Arch Neurol* 65(2):184–189.
7. Voisine C, Pedersen JS, Morimoto RI (2010) Chaperone networks: Tipping the balance in protein folding diseases. *Neurobiol Dis* 40(1):12–20.
8. Nagai Y, Fujikake N, Popiel HA, Wada K (2010) Induction of molecular chaperones as a therapeutic strategy for the polyglutamine diseases. *Curr Pharm Biotechnol* 11(2): 188–197.
9. Pardue S, Groshan K, Raese JD, Morrison-Bogorad M (1992) Hsp70 mRNA induction is reduced in neurons of aged rat hippocampus after thermal stress. *Neurobiol Aging* 13(6):661–672.
10. McCabe T, Simon RP (1993) Hyperthermia induces 72kDa heat shock protein expression in rat brain in non-neuronal cells. *Neurosci Lett* 159(1-2):163–165.
11. Sprang GK, Brown IR (1987) Selective induction of a heat shock gene in fibre tracts and cerebellar neurons of the rabbit brain detected by in situ hybridization. *Brain Res* 427(1):89–93.
12. Mathur SK, et al. (1994) Deficient induction of human hsp70 heat shock gene transcription in Y79 retinoblastoma cells despite activation of heat shock factor 1. *Proc Natl Acad Sci USA* 91(18):8695–8699.
13. Satoh J, Tabira T, Yamamura T, Kim SU (1994) HSP72 induction by heat stress is not universal in mammalian neural cell lines. *J Neurosci Res* 37(1):44–53.
14. Popiel HA, et al. (2012) Hsp40 gene therapy exerts therapeutic effects on polyglutamine disease mice via a non-cell autonomous mechanism. *PLoS ONE* 7(11):e51069.
15. Nagai Y, et al. (2000) Inhibition of polyglutamine protein aggregation and cell death by novel peptides identified by phage display screening. *J Biol Chem* 275(14):10437–10442.
16. Cummings CJ, et al. (1998) Chaperone suppression of aggregation and altered subcellular proteasome localization imply protein misfolding in SCA1. *Nat Genet* 19(2): 148–154.
17. O'Brien MC, Flaherty KM, McKay DB (1996) Lysine 71 of the chaperone protein Hsc70 Is essential for ATP hydrolysis. *J Biol Chem* 271(27):15874–15878.
18. Markova SV, Golz S, Frank LA, Kalthof B, Vysotski ES (2004) Cloning and expression of cDNA for a luciferase from the marine copepod Metridia longa. A novel secreted bioluminescent reporter enzyme. *J Biol Chem* 279(5):3212–3217.
19. Petersen TN, Brunak S, von Heijne G, Nielsen H (2011) SignalP 4.0: Discriminating signal peptides from transmembrane regions. *Nat Methods* 8(10):785–786.
20. Savina A, Furlán M, Vidal M, Colombo MI (2003) Exosome release is regulated by a calcium-dependent mechanism in K562 cells. *J Biol Chem* 278(22):20083–20090.
21. Thery C, Amigorena S, Raposo G, Clayton A (2006) Isolation and characterization of exosomes from cell culture supernatants and biological fluids. *Curr Protoc Cell Biol* Chapter 3:Unit 3.22.
22. Bobrie A, Colombo M, Raposo G, Théry C (2011) Exosome secretion: Molecular mechanisms and roles in immune responses. *Traffic* 12(12):1659–1668.
23. Théry C, Ostrowski M, Segura E (2009) Membrane vesicles as conveyors of immune responses. *Nat Rev Immunol* 9(8):581–593.
24. Trajkovic K, et al. (2008) Ceramide triggers budding of exosome vesicles into multivesicular endosomes. *Science* 319(5867):1244–1247.
25. Pegtel DM, et al. (2010) Functional delivery of viral miRNAs via exosomes. *Proc Natl Acad Sci USA* 107(14):6328–6333.
26. Valadi H, et al. (2007) Exosome-mediated transfer of mRNAs and microRNAs is a novel mechanism of genetic exchange between cells. *Nat Cell Biol* 9(6):654–659.
27. Inouye S, et al. (2003) Activation of heat shock genes is not necessary for protection by heat shock transcription factor 1 against cell death due to a single exposure to high temperatures. *Mol Cell Biol* 23(16):5882–5895.
28. Jackson GR, et al. (1998) Polyglutamine-expanded human huntingtin transgenes induce degeneration of Drosophila photoreceptor neurons. *Neuron* 21(3):633–642.
29. Kazemi-Esfarjani P, Benzer S (2000) Genetic suppression of polyglutamine toxicity in Drosophila. *Science* 287(5459):1837–1840.
30. Nagaraj R, Banerjee U (2007) Combinatorial signaling in the specification of primary pigment cells in the Drosophila eye. *Development* 134(5):825–831.
31. Gross JC, Chaudhary V, Bartscherer K, Boutros M (2012) Active Wnt proteins are secreted on exosomes. *Nat Cell Biol* 14(10):1036–1045.
32. van Oosten-Hawle P, Porter RS, Morimoto RI (2013) Regulation of organismal proteostasis by transcellular chaperone signaling. *Cell* 153(6):1366–1378.
33. Prahlad V, Morimoto RI (2011) Neuronal circuitry regulates the response of Caenorhabditis elegans to misfolded proteins. *Proc Natl Acad Sci USA* 108(34):14204–14209.
34. Hightower LE, Guidon PT, Jr (1989) Selective release from cultured mammalian cells of heat-shock (stress) proteins that resemble glia-axon transfer proteins. *J Cell Physiol* 138(2):257–266.
35. Graner MW, Cumming RI, Bigner DD (2007) The heat shock response and chaperones/heat shock proteins in brain tumors: surface expression, release, and possible immune consequences. *J Neurosci* 27(42):11214–11227.
36. Walsh RC, et al. (2001) Exercise increases serum Hsp72 in humans. *Cell Stress Chaperones* 6(4):386–393.
37. Asea A, et al. (2000) HSP70 stimulates cytokine production through a CD14-dependant pathway, demonstrating its dual role as a chaperone and cytokine. *Nat Med* 6(4): 435–442.
38. Lasek RJ, Gainer H, Barker JL (1977) Cell-to-cell transfer of glial proteins to the squid giant axon. The glia-neuron protein transfer hypothesis. *J Cell Biol* 74(2):501–523.
39. Tytell M, Greenberg SG, Lasek RJ (1986) Heat shock-like protein is transferred from glia to axon. *Brain Res* 363(1):161–164.
40. Zitvogel L, et al. (1998) Eradication of established murine tumors using a novel cell-free vaccine: dendritic cell-derived exosomes. *Nat Med* 4(5):594–600.
41. Villarroya-Beltri C, et al. (2013) Sumoylated hnRNPA2B1 controls the sorting of miRNAs into exosomes through binding to specific motifs. *Nat Commun* 4:2980.
42. Chen T, Guo J, Yang M, Zhu X, Cao X (2011) Chemokine-containing exosomes are released from heat-stressed tumor cells via lipid raft-dependent pathway and act as efficient tumor vaccine. *J Immunol* 186(4):2219–2228.
43. Fujikake N, et al. (2008) Heat shock transcription factor 1-activating compounds suppress polyglutamine-induced neurodegeneration through induction of multiple molecular chaperones. *J Biol Chem* 283(38):26188–26197.

Supporting Information

Takeuchi et al. 10.1073/pnas.1412651112

SI Materials and Methods

Reagents. All reagents were obtained from Sigma unless otherwise specified. siRNAs used for Hsp40 and Hsc70 knockdown were obtained from Santa Cruz Biotechnology and Invitrogen, respectively.

Cell Culture. All of the cell lines used in this study (Neuro2A, SH-SY5Y, U373MG, C6, WT MEF, and HSF1-null MEF) were grown and maintained in DMEM supplemented with 10% (vol/vol) FBS.

Coculture Experiments. Neuro2A cells were transfected with an Hsp40- or Hsp70-encoding plasmid vector using Lipofectamine LTX and PLUS reagent (Invitrogen). Twenty-four hours after transfection, the cells were harvested and plated onto cell culture inserts (Millipore). The culture inserts were then placed above other Neuro2A cells plated on 35-mm glass-bottom dishes (Iwaki), which were transfected with a Q81-EGFP–encoding plasmid for 4 h. These cells were further incubated for 20 h and subjected to microscopic analysis using a confocal microscope (FV1000; Olympus). Cell viability was estimated by counting the viable cells with a Vi-cell XR (Beckman Coulter) cell viability analyzer. Data are shown as the mean ± SEM of at least three experiments.

Plasmid Construction. Plasmid vectors encoding myc-tagged Hsp40 and its deletion mutants (Hsp40-J and Hsp40-GC) were generated by subcloning corresponding fragments from human Hsp40 (DnaJB1) (1) into the EcoRI/BamHI sites of pcDNA3.1 (Invitrogen). Plasmid vectors encoding Hsp70 and its deletion mutant (Hsp70dS) were generated by subcloning corresponding fragments from human Hsp70 (Hspa1a) into the EcoRI/XbaI sites of pCI (Promega). For construction of a plasmid vector encoding Hsp70(K71E), a single-nucleotide mutation (A211G), which corresponds to an amino acid mutation from Lys to Glu at position 71, was introduced in the Hsp70 gene by mutagenesis. The mutated Hsp70 fragment was amplified and inserted into the EcoRI/XbaI sites of pCI, giving an Hsp70(K71E)-encoding vector. Plasmid vectors encoding myc-tagged MetLuc and its deletion mutant (MetLucΔSP) were generated by subcloning corresponding fragments from pMetLuc2-Control (Clontech) into the EcoRI/BamHI sites of pcDNA3.1 (Invitrogen). For construction of a plasmid vector encoding J-MetLucΔSP, a fragment corresponding to MetLucΔSP was amplified by PCR and inserted into the BamHI site of the plasmid vector encoding Hsp40-J (as described above). Plasmid vectors encoding Hsp40/70/90-EYFP were generated by subcloning fragments corresponding to Hsp40/70/90 into the XhoI/BamHI sites of pEYFP-N1 (Clontech).

Preparation of Exosome-Depleted Medium. The depletion of bovine serum-derived exosomes from the medium was performed as described previously (2). Briefly, DMEM containing 10% FBS was centrifuged at 100,000 × *g* for 16 h at 4 °C. The supernatant was sterilized by filtering through a 0.2-μm filter (Millipore) and stored at 4 °C until additional use in exosome preparation.

Preparation of Conditioned Culture Medium and Cell Extracts. Cells were cultured in 35-mm or 100-mm dishes in DMEM containing 10% FBS until 80–90% confluent. The culture medium was then replaced with the exosome-depleted medium. After the indicated incubation times, the culture medium was collected and centrifuged at 3,000 × *g* for 10 min at 4 °C to remove cell debris. For Western blotting, the culture medium was concentrated using 30-kDa cutoff Amicon Ultra filters (Millipore). For the preparation of cell lysates, cells were washed twice with ice-cold PBS and lysed with Tris-buffered saline supplemented with 1% Triton-X 100 on ice for 5 min. The lysed solution was collected and centrifuged to remove cell debris, giving a clear solution of cell lysate. Protein content of the cell lysates was estimated using *DC* Protein Assay (Bio-Rad).

Exosome Isolation from Mouse Serum. Mouse total blood (~5 mo of age) was obtained from the carotid artery under diethyl ether anesthesia. Mouse serum, which was isolated from the total blood, was centrifuged sequentially at 2,000 × *g* for 15 min, 10,000 × *g* for 30 min, and 100,000 × *g* for 120 min. The pellet was resuspended in appropriate buffers.

Western Blotting. Proteins in whole-cell lysates, concentrated culture media, and exosome fractions were separated using 15% or 5–20% gradient SDS/PAGE gels (Wako) and transferred onto PVDF membranes (Bio-Rad). The membranes were incubated overnight with the following antibodies at 4 °C: anti-Alix (ABC40 rabbit polyclonal; Millipore), anti–β-actin (AC-15 mouse monoclonal; Sigma), anti–c-myc (A-14 rabbit polyclonal; Santa Cruz), anti-DnaJA1 (SPA405 rabbit polyclonal; Stressgen), anti-DnaJA2 (3A1 mouse monoclonal; Abcam), anti-DnaJA3 (RS13 mouse monoclonal; Abcam), anti-DnaJB1 (SPA400 rabbit polyclonal; Stressgen), anti-DnaJB6 (B5 mouse monoclonal; Santa Cruz Biotechnology), anti-DnaJC1 (ab81312 rabbit polyclonal; Abcam), anti–Flotillin-1 (C-2 mouse monoclonal; Santa Cruz Biotechnology), anti-GAPDH (IMG-5143A rabbit polyclonal; Imgenex), anti-GFP (A11122 rabbit polyclonal; Invitrogen), anti-Grp78 (610979 mouse monoclonal; BD Biosciences), anti-Hsc70 (SPA816 rabbit polyclonal; Stressgen), anti-Hsp70 (SPA812 rabbit polyclonal, Stressgen; SPA810 mouse monoclonal, Stressgen; SPA820 mouse monoclonal, Stressgen; and d-40 rabbit polyclonal, Santa Cruz Biotechnology), and anti-Hsp90 (SPA830 mouse monoclonal; Stressgen). As secondary antibodies, HRP-conjugated IgGs were used. The HRP signal was visualized with SuperSignal West Dura/Femto Chemiluminescent Substrate (Thermo Fisher Scientific) and captured with a LAS-3000 mini-CCD imaging system (Fujifilm). Acquired images were analyzed with Image J (NIH) software.

Filter Trap Assay. The filter trap assay was performed as previously reported (3). Briefly, Q81-EGFP–expressing cells treated with or without the P100 fraction were lysed with 2% (wt/vol) SDS/PBS, sonicated, and heated at 95 °C, and the lysates were then applied onto a cellulose acetate membrane. The membrane was washed with 2% SDS/PBS and stained with an anti–c-myc antibody (A-14 rabbit polyclonal; Santa Cruz Biotechnology), followed by an HRP-conjugated anti-rabbit secondary antibody.

Immunohistochemistry. Fly heads were fixed in Carnoy's fixative solution, embedded in paraffin, and then sectioned at 3 μm. These sections were deparaffinized and treated with 1% hydrogen peroxide for 30 min and with L.A.B. Solution (Polysciences, Inc.) for antigen retrieval. For the immunoreaction, the sections were pretreated with the blocking solution containing 10% goat serum and then incubated overnight with an anti-GFP antibody at 4 °C, followed by visualization with an EnVision System-HRP (Dako). Hematoxylin was used for counterstaining.

Quantitative RT-PCR. Total RNA was isolated from the bodies (without heads) and the eyes of ~1-wk-old flies (five bodies and 20 eyes per sample, respectively). cDNA was synthesized from total RNA using a PrimeScript RT reagent kit (Takara), and real-time PCR was performed with a 7300 Real-Time PCR System (Applied